Preprints.org

Article

Not peer-reviewed version

Experimental Study on the Influence of Cooling Rates on the Permeability Coefficient of Thawed Soil After Open Frozen

Zhen Wang , Hao-ran Wang , Xiao-hui Ni * , Ming Wu * , Shu Zhu , Semaierjiang Maimaitiyusupu , Zhen-de Zhu

Posted Date: 26 January 2025

doi: 10.20944/preprints202501.1913.v1

Keywords: freezing patterns; cooling rate; artificial ground freezing; thawed soil; permeability coefficient

Preprints.org is a free multidisciplinary platform providing preprint service that is dedicated to making early versions of research outputs permanently available and citable. Preprints posted at Preprints.org appear in Web of Science, Crossref, Google Scholar, Scilit, Europe PMC.

Copyright: This open access article is published under a Creative Commons CC BY 4.0 license, which permit the free download, distribution, and reuse, provided that the author and preprint are cited in any reuse.

Preprints.org (www.preprints.org) | NOT PEER-REVIEWED | Posted: 26 January 2025 doi:10.20944/preprints202501.1913.v1

Disclaimer/Publisher's Note: The statements, opinions, and data contained in all publications are solely those of the individual author(s) and contributor(s) and not of MDPI and/or the editor(s). MDPI and/or the editor(s) disclaim responsibility for any injury to people or property resulting from any ideas, methods, instructions, or products referred to in the content.

Article

Experimental Study on the Influence of Cooling Rates on the Permeability Coefficient of Thawed Soil After Open Frozen

Zhen Wang [1], Hao-ran Wang [1], Xiao-hui Ni [2,*], Ming Wu [1,*], Shu Zhu [3,4], Semaierjiang Maimaitiyusupu [5,6] and Zhen-de Zhu [3,4]

[1] Department of Civil Engineering and Smart Cities, Shantou University, Shantou 515063, China
[2] Jiaxing University College of Civil Engineering and Architecture, Jiaxing 314001, China
[3] Key Laboratory of Ministry of Education for Geomechanics and Embankment Engineering, Hohai University, Nanjing 210098, China
[4] Jiangsu Research Center for Geotechnical Engineering Technology, Hohai University Nanjing 210098, China
[5] College of Civil Engineering, Kashi University, Kashgar 844006, China
[6] College of Water conservancy & Hydropower engineering, Hohai University, Nanjing 210024, China
* Correspondence: nixh2010@zjxu.edu.cn (X.-h.N.); mwu@stu.edu.cn (M.W.)

Abstract: Adjusting freezing patterns is a critical technology in artificial ground freezing (AGF) projects to mitigate frost heave. The distribution of ice lenses formed under varying freezing patterns not only influences frost heave but also modifies the structure of thawed soil, thereby affecting the thaw settlement process. However, most existing research on freezing patterns has primarily focused on their impact on frost heave, with limited attention paid to thaw settlement. This study investigates the cooling rates at the cold side of open frozen systems, which are the key variables defining different freezing patterns, and examines their effect on the permeability coefficient of thawed soil. Experimental results demonstrate that the cooling rate significantly influences the soil permeability coefficient. Specifically, an increase in the cooling rate leads to a reduction in the permeability coefficient, particularly under high frozen temperature conditions. Utilizing the Kozeny-Carman permeability coefficient equation, a predictive model for the permeability coefficient of thawed soil was developed. In practical AGF projects, any freezing pattern can be represented as a combination of different cooling rates. By applying this predictive model, the permeability coefficient of thawed soil under any freezing pattern can be simulated using the corresponding combination of cooling rates. This study provides a valuable reference for predicting thaw settlement following artificial freezing construction.

Keywords: freezing patterns; cooling rate; artificial ground freezing; thawed soil; permeability coefficient

1. Introduction

In artificial ground freezing (AGF) projects, the temperature field of frozen ground is typically unstable and is regulated by the cooling rate of refrigeration systems, resulting in various freezing patterns such as intermittent, stepwise, periodic, or rapid freezing. Engineering practice has demonstrated that these freezing patterns are effective in managing frost heave (H. Ren, Hu, Hong, & Zhang, 2019). However, with the increasing application of AGF in urban expansion projects, it is essential not only to evaluate the effectiveness of freezing patterns on frost heave control, but also to assess thaw settlement control. Because even frost heave is well-controlled by freezing patterns, excessive thaw settlement can lead to serious engineering failures, as illustrated by the thawing settlement incident during the maintenance of the Leaning Tower of Pisa (Leonhardt, 1997). Current research on freezing patterns primarily focuses on their impact on the formation of the temperature

© 2025 by the author(s). Distributed under a Creative Commons CC BY license.

Preprints.org (www.preprints.org) | NOT PEER-REVIEWED | Posted: 26 January 2025 doi:10.20944/preprints202501.1913.v1

field and the evolution of frost heave. There is limited investigation into how these patterns influence thaw settlement, which makes it challenging for engineers to optimize freezing patterns from the perspective of thaw settlement control. Therefore, exploring the effects of different freezing patterns on thaw settlement is essential for selecting the most appropriate freezing patterns. The permeability coefficient is a critical parameter that influences the settlement and deformation of thawed soil (J. Zhou & Tang, 2015). This paper aims to examine the changes in the permeability coefficient of thawed soil under various freezing patterns through experiments, thereby elucidating the mechanism by which freezing patterns affect thawing settlement.

Currently, many valuable findings have been obtained regarding the impact of freezing patterns on temperature fields and frost heave in AGF. For example, Sun et al. (Sun, Wang, Guo, Song, & Wang, 2024) found that during the freezing process, frost heave in soil is significantly influenced by the cooling rate of the cold side of open frozen(the cooling rate of refrigeration). Under the same conditions, a higher cooling rate results in faster downward movement of the freezing front and smaller frost heave in the soil. Wu et al. (Wu, 2021) compared linear cooling and constant freezing temperature of the cold side of open frozen(the temperature of refrigeration) and discovered that linear cooling is more conducive to the occurrence of frost heave compared to constant freezing temperature. Zhou et al. (Y. Zhou & Zhou, 2012) found that intermittent freezing of the cold side of open frozen results in less frost heave than continuous freezing, attributing this to the backward movement of the freezing front, which causes the disappearance of the frozen fringe, stops the growth of the final ice lens. Bing et al. (Hui & Ping, 2009) observed that in cyclic freezing of the cold side of open frozen, the amount of frost heave in each cycle decreases with an increase in the number of freeze-thaw cycles. Despite these findings, research on the influence of freezing patterns on thaw settlement remains insufficient. Consequently, current findings are primarily applicable to evaluating frost heave in engineering contexts and cannot adequately assess the effects on thaw settlement. From the perspective of controlling AGF deformation, it remains unclear which freezing pattern is most effective in mitigating thaw settlement.

In the domain of thawed soil permeability, research indicates that the permeability of thawed soil is influenced by various factors, including soil properties (C. Chen et al., 2023; Li et al., 2023; Lv et al., 2021; Xu, Wang, Ren, & Yuan, 2016; H. Zhang, Zhang, Zhang, & Chai, 2016; L. Zhang, 2022) and other factors such as unsaturated soil , multiple freeze-thaw effects (Chamberlain, 1990; Viklander, 1998), alternating dry and wet conditions (L. Zhang, Liao, & Wang, 2023), and the compression(Bao, Xue, Zhang, Dai, & Cui, 2020). However, most of these studies were conducted in the condition of closed freezing. There is a fundamental distinction between open frozen and closed freezing, and AGF is a typical example of the open frozen type. Consequently, existing research findings on permeability provide limited guidance for AGF. Yang et al. (Yang & Zhang, 2002) investigated the effect of freeze-thaw cycles on the permeability of clay under open frozen conditions and found that the permeability of thawed soil can increase by more than an order of magnitude. Wang (Wang, 2009) found that under the same freezing temperature conditions, the increase in permeability coefficient for open frozen is greater than that for closed freezing. Go et al. (Hirose & Ito, 2017) investigated the influence of horizontal and vertical freezing on the permeability of thawed soil in open frozen conditions. Zeina et al. (Joudieh, Cuisinier, Abdallah, & Masrouri, 2024) found that compressive stress during open frozen can mitigate the increase in the permeability of thawed soil. An et al. (An, Kong, & Li, 2020) studied the effect of the frozen temperature in open frozen on the permeability coefficient of thawed soil, finding that lower freezing temperatures lead to a more significant increase in permeability. Despite these findings, research specifically examining the impact of open freezing patterns on the permeability coefficient of thawed soil remains limited.

In actual AGF, a combination of various freezing patterns is typically employed rather than a single, specific pattern. Replicating all possible freezing patterns in a laboratory setting to understand these combinations is virtually impossible. Therefore, the focus should shift to understanding the underlying principles governing different freezing patterns. It is crucial to note that any freezing pattern is defined by the cooling rates at the cold side of the open freezing system (the cooling rate of

Preprints.org (www.preprints.org) | NOT PEER-REVIEWED | Posted: 26 January 2025 doi:10.20944/preprints202501.1913.v1

refrigeration). For example, stepwise freezing involves an initial high cooling rate followed by a period with no change in the cooling rate, while intermittent freezing consists of alternating cycles of linear cooling and heating. Cyclic freezing comprises multiple stepwise freezing cycles. By understanding how cooling rates at the cold side influence the permeability coefficient of thawed soil, we can simulate any practical freezing pattern by adjusting these cooling rates. However, research on the impact of cooling rates on the permeability coefficient of thawed soil remains limited.

This paper aims to experimentally investigate the impact of cooling rates on the permeability coefficient of thawed soil, elucidating the mechanisms behind thaw settlement in AGF. The findings of this study will improve the accuracy of thaw settlement predictions in AGF projects and provide a theoretical foundation for better control of thaw settlement, thereby ensuring safe construction in complex underground environments.

2. Test Apparatus

2.1. The Semiconductor-Based Open Frozen System (SOF)

AGF is an open freezing process, which differs from natural freezing, and typically involves ultra-low freezing temperatures and rapid freezing (such as liquid nitrogen freezing). Therefore, laboratory investigations into the impact of cooling rates of AGF must simulate conditions that incorporate both rapid cooling and ultra-low temperatures. Currently, in laboratory studies, controlled flow rates of liquid nitrogen can achieve rapid cooling and ultra-low temperatures. However, maintaining a constant cooling rate over an extended period and achieving high-precision control of the cooling rate remain challenging. To address this issue, we have developed a new open freezing system based on semiconductors, known as the SOF freezing system (Figure 1). This system utilizes a combination of semiconductor and compressor cooling, enabling precise control and switching of the cooling rates (from 1°C/s to 1°C/h). It is characterized by high stability and precision (±0.01°C/s) and can achieve temperatures as low as -90°C.

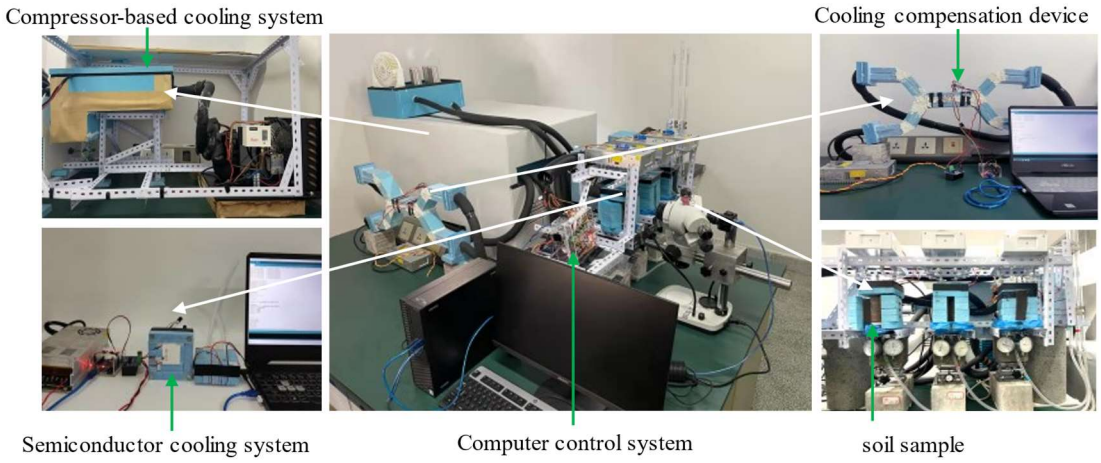

Figure 1. The semiconductor-based open frozen system (SOF). It consists of three main components: 1. Compressor-based cooling system; 2. Semiconductor cooling system; 3. Computer control system.

The SOF freezing system relies on the collaboration between semiconductors and compressor-based refrigeration, as shown in Figure 2. The system comprises three stages of refrigeration. In the first stage, compressor-based refrigeration creates a low-temperature environment for the semiconductor. The third stage involves the semiconductor directly freezing the soil sample, with heat generated by the semiconductor being transferred to the compressor-based refrigeration. The cooling rate is controlled by the electrical regulation of the semiconductors. However, when the cooling rate of the semiconductor changes too rapidly, the refrigeration compressor struggles to

Preprints.org (www.preprints.org) | NOT PEER-REVIEWED | Posted: 26 January 2025 doi:10.20944/preprints202501.1913.v1

maintain temperature stability due to thermal shock. To address this, a high-speed response cooling compensation device, also based on semiconductors, has been incorporated into the compressor-based refrigeration system as the second stage. Typical cooling rates for the system are depicted in Figure 3.

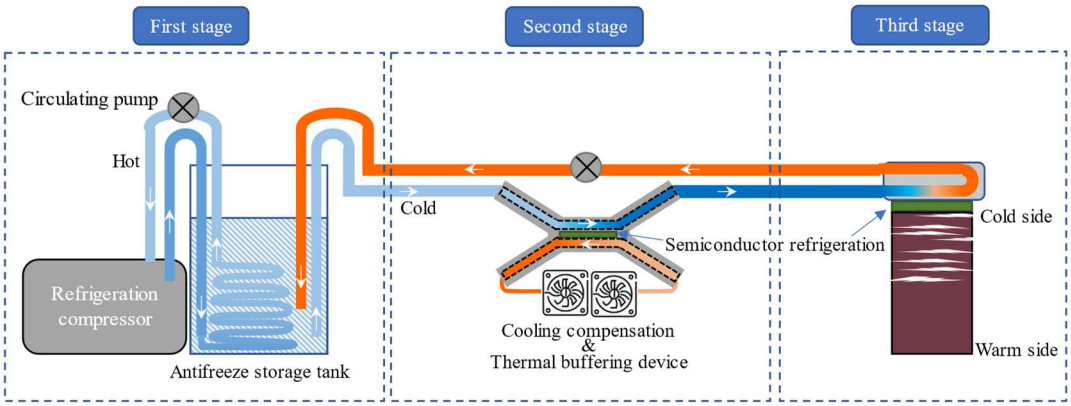

Figure 2. Schematic diagram of the working principle of the SOF freezing system.

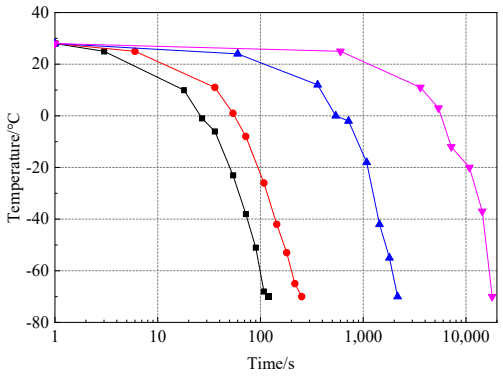

Figure 3. The typical temperature change curve of the SOF freezing system.

2.2. Independently Developed Variable-Head Permeameter

The uneven distribution of ice lenses within frozen soil leads to varying permeability across different locations of the thawed soil sample. To accurately assess the permeability of thawed soil, samples must be collected from multiple positions, with each position's permeability coefficient measured individually. For this purpose, an independently developed variable-head permeameter was employed in this experiment to measure the permeability coefficients of thawed soil collected from different positions of original sample, which had a reduced height after being sectioned. This instrument is specifically designed to accommodate the dimensions of the thawed soil samples post-sectioning, as illustrated in Figure 4

Preprints.org (www.preprints.org) | NOT PEER-REVIEWED | Posted: 26 January 2025 doi:10.20944/preprints202501.1913.v1

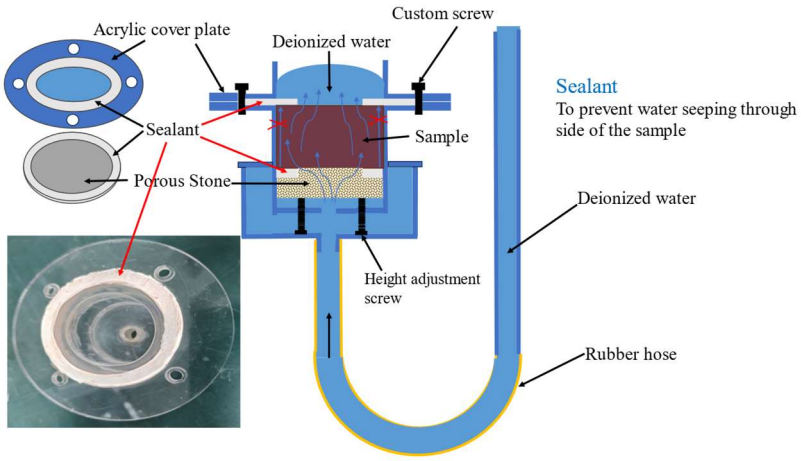

Figure 4. Independently developed variable-head permeameter.

The sample chamber of the permeameter is made of acrylic material. Sealant is applied to the edges of the acrylic cover plate and the porous stone to prevent water from seeping through the sides of the sample, as shown in Figure 4. A height adjustment screw, located beneath the porous stone, compensates for the size of the thawed soil samples after sectioning, as well as the vertical shrinkage that occurs when the frozen soil thaws. By adjusting this screw, the top of the thawed soil sample maintains tight contact with the sealant.

2.3. Microscopy-Based Ice Lens Measure System (MIL)

The ice lens is a critical microstructure in open freezing processes, and understanding its distribution is essential for elucidating the microscale mechanisms that govern the evolution of permeability coefficients. Ice lenses are highly sensitive to temperature, making it crucial to minimize temperature disturbances during observation. Ideally, in situ observation of ice lenses would be preferable; however, conventional techniques such as Computed Tomography (CT), Nuclear Magnetic Resonance (NMR), and Scanning Electron Microscope (SEM) face significant challenges in minimizing temperature disturbances. To address this issue, we have developed a novel microscopy-based ice lens measurement system (MIL), shown in Figure 5, which employs microscopic digital imaging technology to observe ice lenses at a microscale. Notable features of the MIL include a wide operating temperature range and a compact design. When coupled with the SOF freezing system, the MIL allows for in-situ and continuous observation of ice lenses.

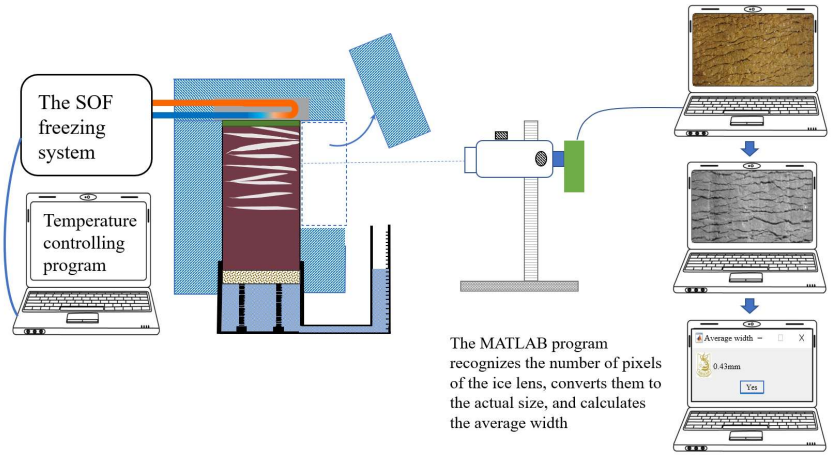

Figure 5. The microscopy-based ice lens measure system (MIL).

Preprints.org (www.preprints.org) | NOT PEER-REVIEWED | Posted: 26 January 2025 doi:10.20944/preprints202501.1913.v1

The mechanism of the MIL operates as follows: at a fixed magnification, each pixel in the digital camera image corresponds uniquely to the physical dimensions of the object. By statistically analyzing the pixel values of the ice lens, the actual dimensions can be calculated. As shown in Figure 6, given a known area A and observed pixel value M, the area represented by a single pixel (T1) at a magnification (L1) is T1 = A/M. At this constant magnification (L1), if the pixel count of an object is C, the corresponding area B can be determined as B = T1*C. The table in Figure 6 displays the pixel areas at different magnifications.

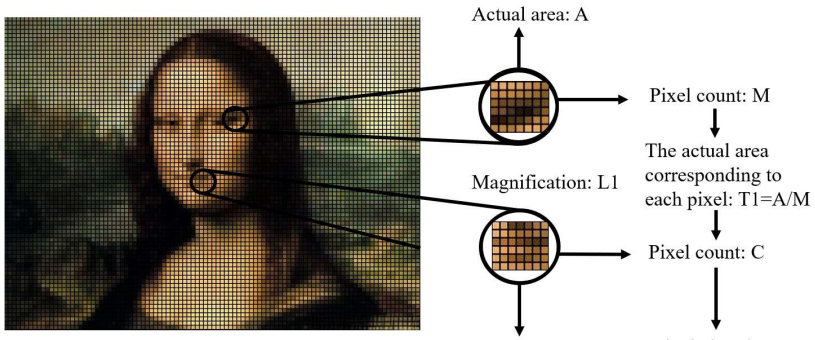

Magnifi -cation	Actual value of X×Y（mm）	Corresponding pixel value	Unit pixel size（mm）
10	10×5.5	1920×1080	0.00521×0.00509
15	6×3.5	1920×1080	0.00313×0.00324
20	5×2.5	1920×1080	0.00260×0.00231
30	3×2	1920×1080	0.00156×0.00185
40	2.5×1.5	1920×1080	0.00130×0.00139
45	2×1	1920×1080	0.00104×0.00093

At the same magnification, the actual size corresponding to each pixel remains constant. The actual sizes corresponding to each pixel at different magnifications are shown in the table.

Figure 6. The work principle of the MIL measure system.

3. Experimental Scheme

3.1. Experimental Design

The soil sample used in this study was collected from silty clay in the Jinping District, Shantou City. The grain size distribution curve of the clay is shown in Figure 7. The liquid limit is 43%; the plastic limit is 20%; the density is 1.75 g/cm^3 and saturation of 84.08%. The soil sample is a standard cylindrical specimen with a diameter of 39.1 mm and a height of 80 mm.

The experiment consists of two main parts: open freezing experiment and permissibility experiment.

In the open freezing experiment, the sample is placed vertically inside the sample chamber. The chamber is equipped with an insulating layer, as shown in Figure 8. The temperature at the cold side of open frozen are set to -35°C, -55°C, and -75°C, with cooling rates of 0.5°C/s, 0.05°C/s, and 0.005°C/s, respectively. The freezing duration is 12 hours. At the warm side of open frozen water replenishment pressure is set as 0.2 kPa and 0.02 kPa. A total of 18 different test conditions are designed, with each group containing 4 samples, resulting in a total of 72 samples, as outlined in Table 1.

In the permissibility experiment, the frozen soil sample is cut near the cold side to a size of 23 mm. Then the intercepted sample is placed in the sample chamber of the variable-head permeameter and allowed to thaw for 12 hours at room temperature inside the sample chamber. By adjusting the height adjustment screw, the top of the thawed soil sample is kept in tight contact with the sealant. Subsequently, a permeability test is performed to measure the vertical permeability coefficient of the thawed soil in segments, as shown in Figure 8.

Preprints.org (www.preprints.org) | NOT PEER-REVIEWED | Posted: 26 January 2025 doi:10.20944/preprints202501.1913.v1

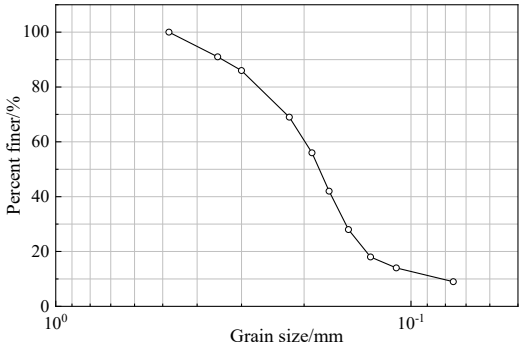

Figure 7. The grain size distribution curve.

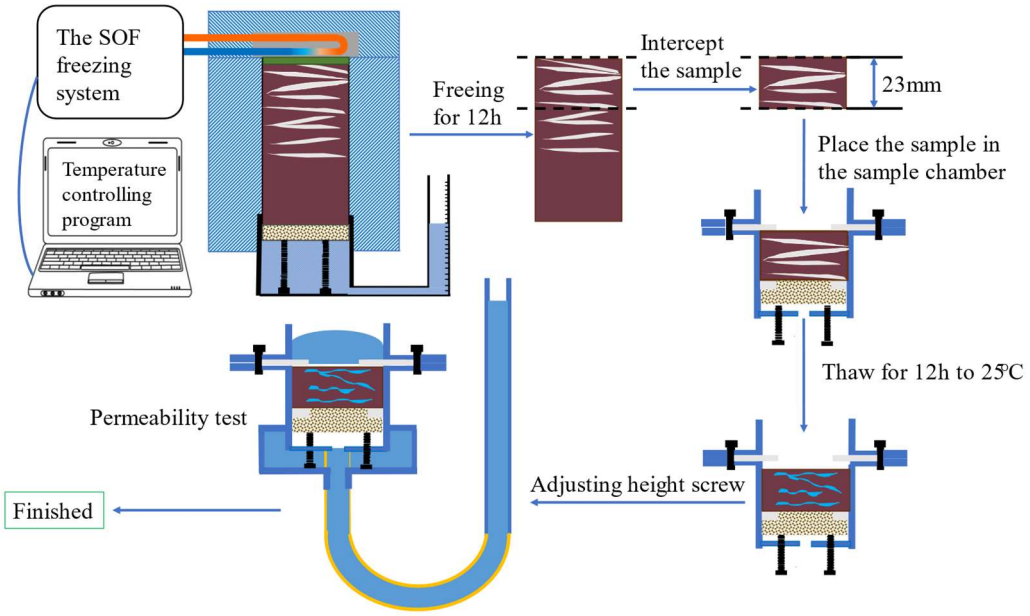

Figure 8. Test design diagram.

Table 1. Freezing boundary conditions.

Frozen temperature (℃)	Cooling rate (℃/s)	Water replenishment pressure (kPa)
-35	0.5	0.2
-55	0.05	
-75	0.005	0.02

3.2. Experimental Procedure

The experimental procedure comprises three main stages: sample preparation, open freezing experiment, and permeability experiment, as illustrated in Figure 9.

Preprints.org (www.preprints.org) | NOT PEER-REVIEWED | Posted: 26 January 2025 doi:10.20944/preprints202501.1913.v1

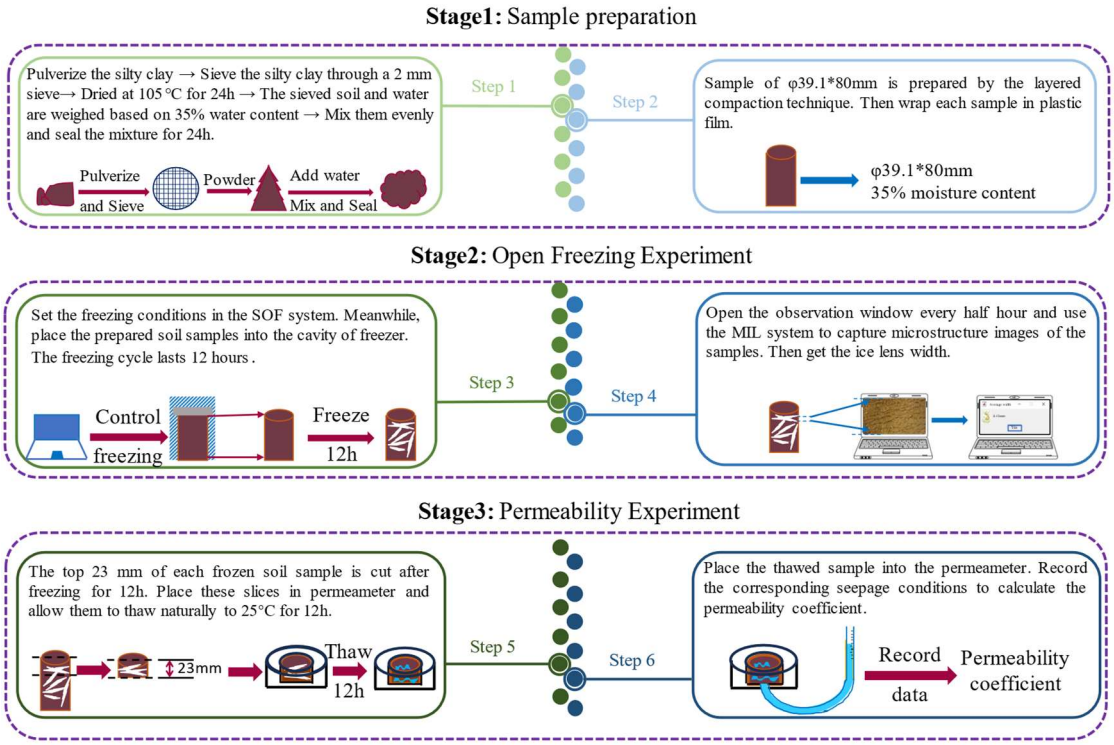

Figure 9. Experimental procedure.

3.2.1. Sample Preparation

The sample preparation process is crucial for ensuring the accuracy the experimental results. The following steps outline the procedures for soil preparation, water content adjustment, and sample production:

1. Soil Preparation: The soil is initially crushed to break down large clumps, then sieved through a 2mm screen to remove larger particles and debris. The sieved soil is subsequently dried in an oven at 105°C for 24 hours to eliminate excess moisture, ensuring a consistent starting condition for the experiment.
2. Water Content Adjustment and Homogenization: To achieve uniform water content across all samples, a specific amount of water is added to the dried soil to reach a target water content of 35%. The mixture is then thoroughly mixed using a mechanical mixer to ensure homogeneity. Afterward, the mixed soil sample is sealed in airtight containers and stored for 24 hours to allow the water to evenly distribute throughout the soil matrix.
3. Sample Preparation: The layered compaction technique is used to prepare cylindrical specimens with a diameter of 39.1 mm and a height of 80 mm. Each specimen is immediately wrapped in plastic film to protect it from environmental factors during handling.

3.2.2. Open Freezing Experiment

The open freezing experiment is conducted using both the SOF and MIL systems. The detailed steps for conducting this experiment are as follows:

1. Equipment Setup: Set the required frozen temperature and cooling rate in the SOF system.
2. Sample Placement and Experiment Start: Carefully place the prepared soil samples into the freezer cavity and set the appropriate water replenishment pressure. Initiate the freezing process.
3. Monitoring and Recording: Throughout the experiment, the observation window of the cavity is briefly opened every half hour for approximately 5 seconds. During this time, the MIL system is used to capture microstructural images of the samples, enabling real-time monitoring of

Preprints.org (www.preprints.org) | NOT PEER-REVIEWED | Posted: 26 January 2025 doi:10.20944/preprints202501.1913.v1

changes within the soil's microstructure. The entire freezing cycle lasts 12 hours, generating a comprehensive dataset for analysis.

3.2.3. Permeability Experiment

Following the freezing stage, the permeability coefficient of the soil samples is measured using an independently developed variable-head permeameter. The procedure for this test is as follows:

1. Preparation: After the freezing stage, the top 23 mm of each frozen soil sample is precisely cut using a wire saw to obtain test samples.
2. Instrument Setup: Place these slices into the variable-head permeameter and allow them to thaw naturally at room temperature (25°C). It should be noted that volume changes during the melting process may occur, potentially separating the sample from the top sealant.
3. Adjustment and Measurement: Adjust the height adjustment screws to ensure that the thawed soil is in close contact with the top sealant ring. Vary the water pressure and record the corresponding seepage conditions to calculate the permeability coefficient.

4. Results and Discussions

4.1. Experimental Results of Permeability Coefficient

Table 2 presents the experimental results of the permeability coefficients for 18 different combinations of frozen boundary conditions.

Table 2. The permeability coefficient.

Group number	Frozen temperature (℃）	Cooling rate (℃/s）	Water replenishment pressure (kPa)	Permeability coefficient (10^-6)
1	-35	0.5	0.02	5.343
2	-35	0.05	0.02	10.430
3	-35	0.005	0.02	13.950
4	-35	0.5	0.2	5.9431
5	-35	0.05	0.2	10.8363
6	-35	0.005	0.2	14.2531
7	-55	0.5	0.02	3.890
8	-55	0.05	0.02	6.930
9	-55	0.005	0.02	11.690
10	-55	0.5	0.2	3.8984
11	-55	0.05	0.2	7.8010
12	-55	0.005	0.2	11.6972
13	-75	0.5	0.02	1.170
14	-75	0.05	0.02	5.230
15	-75	0.005	0.02	8.260
16	-75	0.5	0.2	3.5238
17	-75	0.05	0.2	7.2531
18	-75	0.005	0.2	8.4256

The permeability coefficients from Table 2 are represented by bubbles in Figure 10, where larger and darker bubbles indicate higher permeability values. Figure 10 illustrates that, in addition to traditional open freezing boundary conditions such as temperature gradient and water replenishment pressure, the cooling rate also affects the permeability of thawed soil. As the cooling rate decreases, the temperature gradient diminishes, and the water replenishment pressure increases, leading to a gradual rise in the permeability coefficient of the thawed soil. The maximum permeability coefficient is observed when both the cooling rate and temperature gradient are at their lowest, and the water replenishment pressure is at its highest. This finding suggests that, in practical

Preprints.org (www.preprints.org) | NOT PEER-REVIEWED | Posted: 26 January 2025 doi:10.20944/preprints202501.1913.v1

AGF applications, high cooling rates, large temperature gradients, and low water replenishment pressures help reduce the permeability of thawed soil.

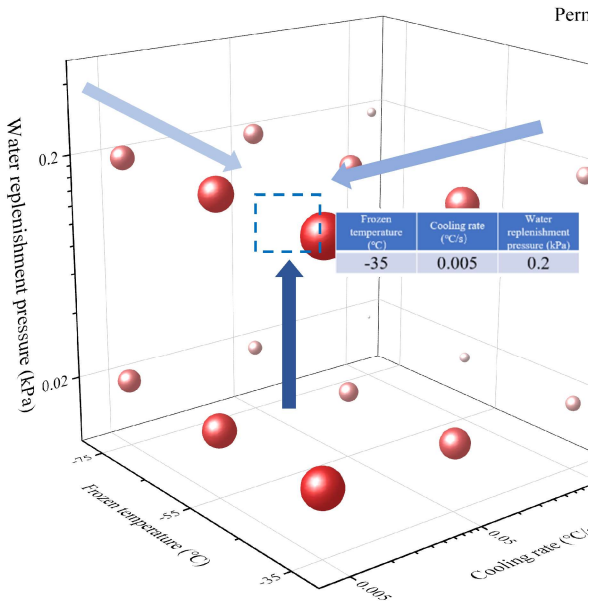

Figure 10. A three-dimensional bubble plot of the permeability coefficients. Larger and darker bubbles represent higher permeability coefficients.

4.2. The Influence of Cooling Rate and Temperature Gradient on the Permeability

Although the cooling rate, temperature gradient, and water replenishment pressure all significantly impact the permeability coefficient of thawed soil, the primary focus for adjusting the freezing pattern in engineering is modifying the cooling rate and temperature gradient. Therefore, it is crucial to analyze the combined effect of these two factors on the permeability coefficient under a constant water replenishment pressure.

Under a water replenishment pressure of 0.2 kPa, the permeability coefficients listed in Table 2 are depicted in a two-dimensional heatmap, as shown in Figure 11.

Preprints.org (www.preprints.org) | NOT PEER-REVIEWED | Posted: 26 January 2025 doi:10.20944/preprints202501.1913.v1

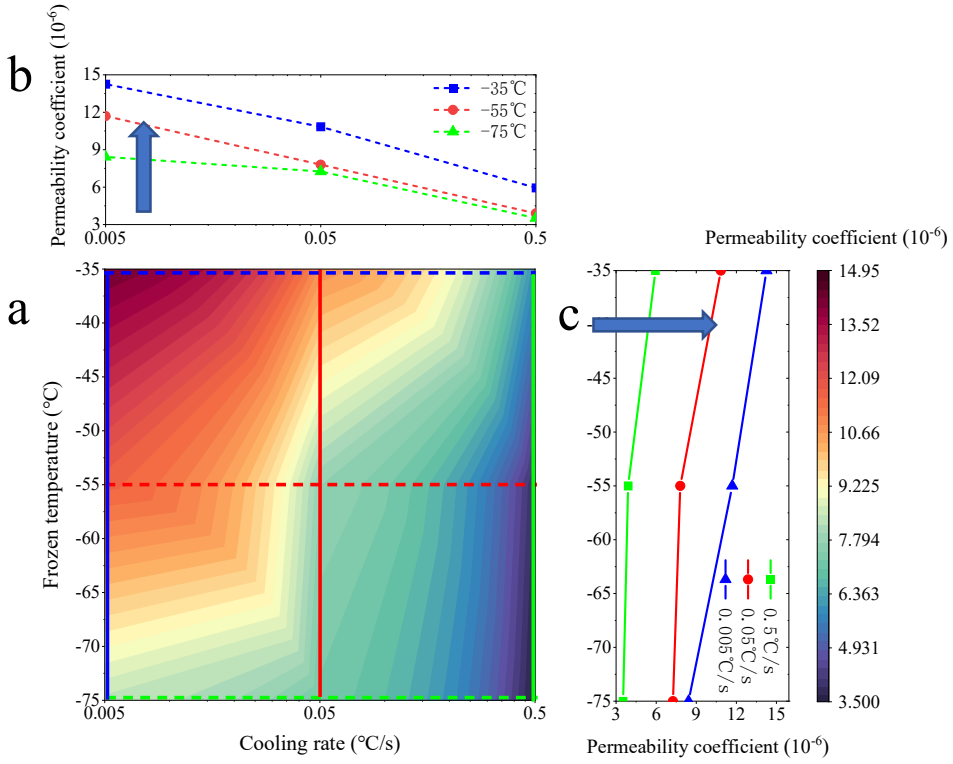

Figure 11. Permeability coefficient under the condition of a water replenishment pressure of 0.2KPa.

The maximum permeability coefficient is observed in the upper-left corner of Figure 11 (a), where both the freezing temperature gradient and cooling rate are at their minimum. A smaller temperature gradient and lower cooling rate result in an increased permeability coefficient of the thawed soil. Currently, intermittent freezing is a common method for controlling frost heave in engineering. To mitigate settlement during intermittent freezing, based on the experimental results, the cooling rate should be increased in each freezing stage. This requires enhancing the power of the freezing equipment to achieve a higher cooling rate. The same principle applies to other cooling methods: increasing the temperature gradient and cooling rate helps control settlement caused by these methods.

By comparing the lower-left and lower-right corners of Figure 11 (a), it is evident that increasing the cooling rate under a constant temperature gradient can effectively reduce the permeability coefficient. The dotted lines in Figure 11 (a) represent permeability coefficients at three fixed temperature gradients: -35°C, -55°C, and -75°C (these coefficients are reorganized in Figure 11 (b)). In Figure 11 (b), these lines demonstrate that, regardless of the constant temperature gradient, increasing the cooling rate results in a reduction of the permeability coefficient. This suggests that in practical engineering, when the frozen temperature of the freezing equipment cannot be further reduced, accelerating the cooling rate can decrease the permeability coefficient and help control thaw settlement.

However, it is important to note that the reduction in permeability due to an increase in cooling rate varies with different temperature conditions, with the most significant reduction occurring at -35°C. This indicates that, under high-temperature freezing conditions, increasing the cooling rate leads to a more substantial reduction in permeability. Currently, most AGF systems use brine as a coolant and operate under high-temperature freezing conditions, where increasing the cooling rate is particularly effective for managing thaw settlement.

By comparing the top-right and bottom-right corners of Figure 11 (a), it is clear that, when the cooling rate is constant, increasing the temperature gradient alone can also reduce the permeability coefficient. The solid lines in Figure 11 (a) represent permeability coefficients under three different cooling rates: 0.5°C/s, 0.05°C/s, and 0.005°C/s (these coefficients are reorganized in Figure 11 (c)). In

Preprints.org (www.preprints.org) | NOT PEER-REVIEWED | Posted: 26 January 2025 doi:10.20944/preprints202501.1913.v1

Figure 11 (c), these data show that enhancing the temperature gradient effectively suppresses the increase in permeability, regardless of the constant cooling rate. Therefore, if it is not possible to increase the cooling rate in a project, a similar effect can be achieved by increasing the temperature gradient.

However, the response to the same increase in temperature gradient varies with different cooling rates. As shown in Figure 11 (c), the effect of increasing the temperature gradient is more pronounced at 0.005°C/s, indicating that a greater reduction in the permeability coefficient occurs during slower freezing. Given that the freezing equipment in current projects generally has low power, adjusting the temperature gradient may be a key strategy for improving the management of thaw settlement.

5. Micro-Mechanism of the Evolution of Permeability Coefficient

5.1. The Effect of Cooling Rate

From a macroscopic standpoint, an increase in the cooling rate typically results in a reduction in the permeability coefficient of thawed soil. This inverse relationship, however, is not entirely understood at the microscopic level. To better comprehend the underlying physical mechanisms, we examined microstructural images of ice lenses in frozen soil under controlled conditions of constant temperature gradient and water replenishment pressure, as shown in Figure 12.

The images reveal a notable trend: as the cooling rate increases, the width of the ice lenses decreases. Upon thawing, these ice lenses act as conduits, creating channels that allow water to flow through the thawed soil. The width of these ice lenses is crucial in determining the resistance to the closure of these channels during the thaw-settlement process. When the ice lenses are wider, they hinder the complete closure of these channels, allowing more unimpeded water flow and, in turn, a higher permeability coefficient. Conversely, narrower ice lenses facilitate a more effective closure of these channels, reducing water flow and lowering the permeability coefficient.

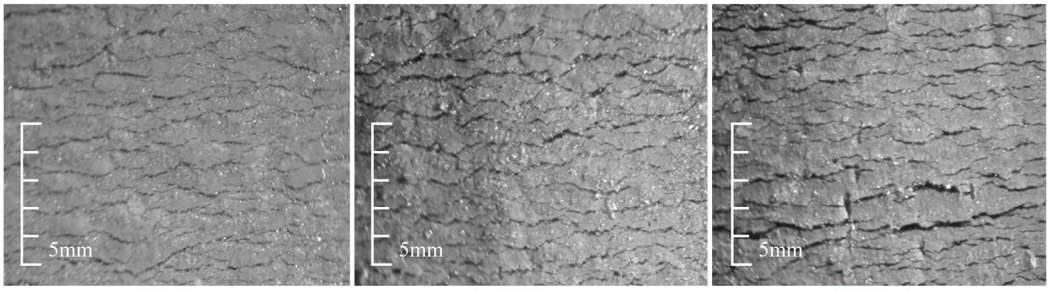

Figure 12. The variation in ice lens width under different cooling rates.

5.2. The Effect of Temperature Gradient

In addition to cooling rate, the temperature gradient plays a critical role in influencing the permeability coefficient of thawed soil. Figure 13 presents microstructural images of ice lenses in frozen soil under constant cooling rates and water replenishment pressure conditions. The observations indicate that as the temperature gradient increases, the width of the ice lenses decreases significantly. This narrowing of ice lenses suggests that a higher temperature gradient promotes a more rapid freezing process, which limits the growth of the ice lenses and restricts the formation of large channels through the thawed soil.

The implication of this finding is clear: a higher temperature gradient leads to a reduced permeability coefficient of the thawed soil. This is because the narrower ice lenses, resulting from a steeper temperature gradient, are more likely to facilitate a more complete closure of the water

Preprints.org (www.preprints.org) | NOT PEER-REVIEWED | Posted: 26 January 2025 doi:10.20944/preprints202501.1913.v1

channels during thawing. As a result, water flow through the thawed soil is more effectively restricted, reducing permeability.

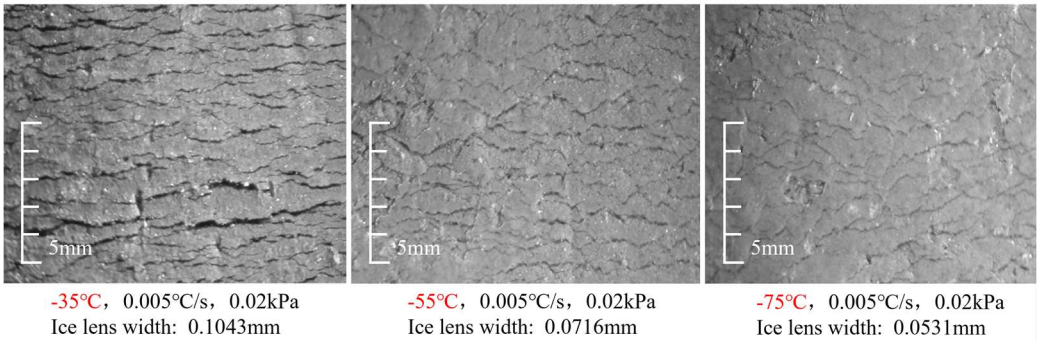

Figure 13. The variation in ice lens width under different temperature gradient.

5.3. The Effect of Water Replenishment Pressure

Another important factor that influences the permeability coefficient of thawed soil is water replenishment pressure. Under constant temperature gradient and cooling rate conditions, we observed the evolution of ice lenses in frozen soil, as shown in Figure 14. As the water replenishment pressure increases, the width of the ice lenses also increases. This suggests that higher water replenishment pressure promotes the formation of larger ice lenses during the freezing process, which in turn creates larger channels for water flow during thawing.

Larger ice lenses result in less resistance to the closure of these channels during the thaw-settlement process, leading to more unobstructed water flow. Consequently, a higher water replenishment pressure results in a higher permeability coefficient of the thawed soil. This observation aligns with the general understanding that higher pressure can promote the formation of more permeable soil structures by facilitating the growth of ice lenses and thereby increasing the size of water-conducting channels.

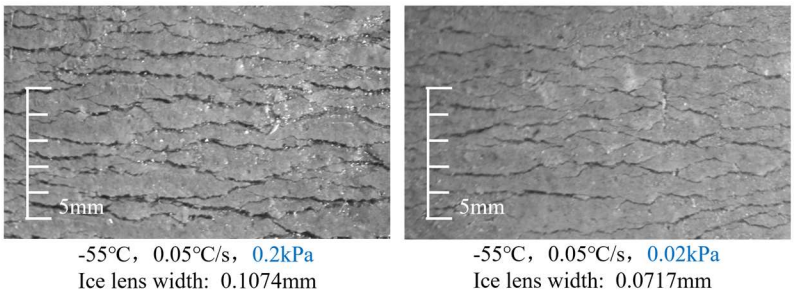

Figure 14. The variation in ice lens width under different water replenishment pressure.

6. Permeability Coefficient Prediction Model

6.1. The Permeability Coefficient Prediction Model Based on the Kozeny-Carman Equation

As discussed in Section 4.1, the permeability coefficient of thawed soil is influenced by several macro-variables, including the temperature gradient, water replenishment conditions, and cooling rate. Therefore, it is theoretically feasible to develop a regression analysis model that utilizes these parameters to predict the permeability coefficient of thawed soil.

The Kozeny-Carman equation is widely used in the study of permeability coefficients, as it provides a robust method for estimating the permeability of porous media, such as soil and rock(J. Chen, Tong, Yuan, Fang, & Gu, 2022; X. Ren et al., 2016). The equation is expressed as follows:

Preprints.org (www.preprints.org) | NOT PEER-REVIEWED | Posted: 26 January 2025 doi:10.20944/preprints202501.1913.v1

$$\mathrm{k} = \frac{c_2 \rho_{wz} e^3}{s^2 \eta (1+e)} \tag{1}$$

Where, k is the permeability coefficient (cm/s). e is the porosity of the soil. ρ_{wz} is the density of free water (g/cm³). c_2 is a parameter related to the particle shape and the actual flow direction of the water. s is the specific surface area of the soil particles (cm⁻¹). η is the dynamic viscosity of free water (g·s·cm⁻²).

Equation (1) can be rewritten as:

$$c_2 = \frac{\mathrm{k} s^2 \eta (1+e)}{\rho_{wz} e^3} \tag{2}$$

In this paper, the specific surface area of the soil $s = 4.1586 \times 10^3 cm^{-1}$. The porosity of the soil $e = 0.75$ .The dynamic viscosity of free water $\eta = 3.34 \times 10^{-4} g \cdot s \cdot cm^{-2}$. The density of free water $\rho_{wz} = 0.9584 g/cm^3$ .Substituting these values into Equation (2) yields the quantitative relationship between the permeability coefficient k and c_2 as:

$$c_2 = 2.50004726 * 10^4 k \tag{3}$$

After reviewing the experimental data from Table 2, the c_2 corresponding to the permeability coefficient k for each test were calculated,

Assuming that parameter c_2 is no longer a constant in soil melting, but a function with frozen temperature, cooling rate, and water replenishment pressure and satisfying the following relationship:

$$c_2 = \mathrm{AT} + \mathrm{B} \lg \mathrm{V} + \mathrm{C} \lg \mathrm{P} + \mathrm{D} \tag{4}$$

Where，T is frozen temperature. V is cooling rate. P is water replenishment pressure. A. B, C, D are undetermined parameters. Reviewing the c_2 data calculated from Equation(3), after performing regression analysis, the following parameter values were obtained: A = 0.00280, B = -0.09273, C = 0.01872, and D = 0.25106.

Substituting these parameters into the Kozeny-Carman equation, we obtain the permeability coefficient prediction model as follows:

$$\mathrm{k} = \frac{\rho_{wz} e^3}{s^2 \eta (1+e)} (0.00280T - 0.09273 \lg V + 0.01872 \lg P + 0.25106) \tag{5}$$

This prediction model incorporates three freezing boundary conditions—frozen temperature (T), cooling rate (V), and water replenishment pressure (P)—to describe the parameter c_2, which is related to particle shape and the actual flow direction of water. This approach enhances the applicability of the Kozeny-Carman equation under open freezing conditions and can serve as a reference for predicting permeability coefficients in practical AGF projects.

This prediction model incorporates three key boundary conditions—frozen temperature (T), cooling rate (V), and water replenishment pressure (P)—to describe the parameter c_2, which is related to particle shape and the flow characteristics of water. This adaptation of the Kozeny-Carman equation enhances its applicability under open freezing conditions, making it a practical tool for predicting permeability coefficients in real-world applications, such as in AGF projects.

6.2. Model validation

To validate the accuracy and applicability of the permeability coefficient prediction model under various freezing boundary conditions, additional experiments were conducted. These tests were

Preprints.org (www.preprints.org) | NOT PEER-REVIEWED | Posted: 26 January 2025 doi:10.20944/preprints202501.1913.v1

designed to cover a range of freezing conditions, as detailed in Table 3. The experimental setup included variations in frozen temperature, cooling rate, and water replenishment pressure to test the robustness of the model.

Table 3. Freezing boundary conditions of model validation.

Group number	Frozen temperature (℃)	Cooling rate (℃/s)	Water replenishment pressure (kPa)
1	-40	0.1	0.01
2	-60	0.1	0.01
3	-60	0.01	0.1
4	-60	0.1	0.1

The experimental results are shown in Figures 15 and 16.

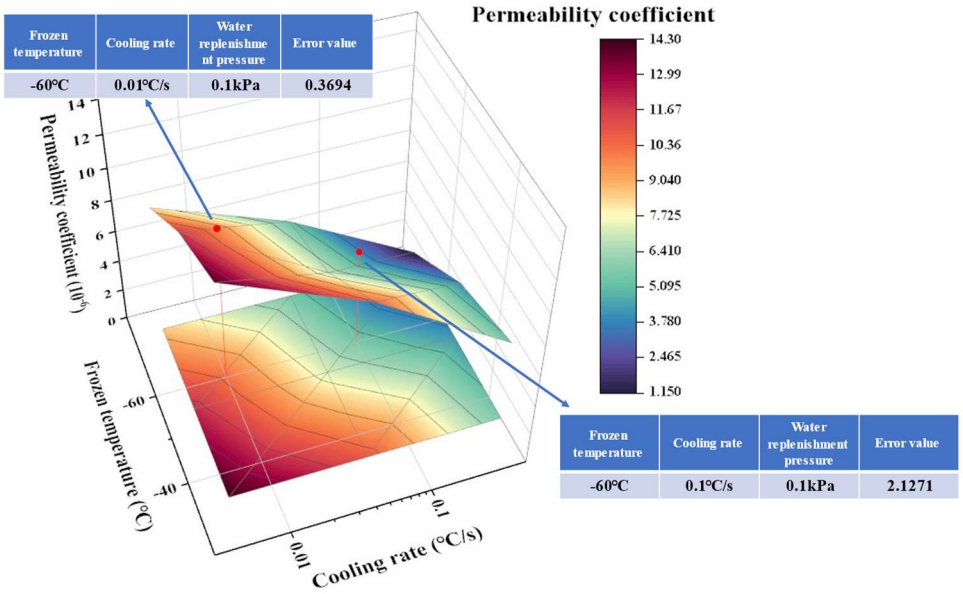

Figure 15. Comparison of predicted and experimental values of the permeability coefficient at a water replenishment pressure of 0.1 kPa. The surface represents the predicted values, while the red dots indicate the experimental data points.

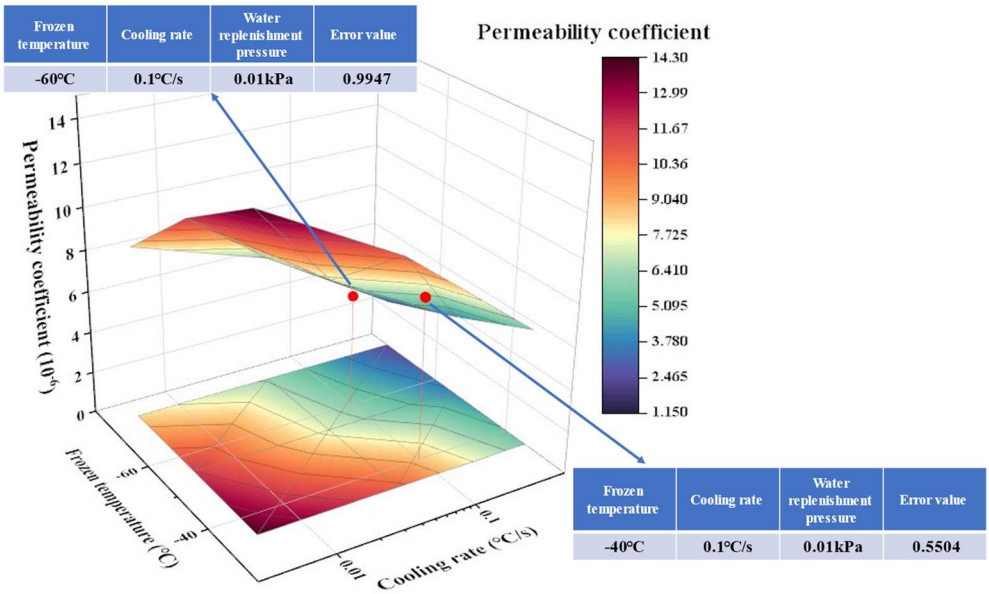

Preprints.org (www.preprints.org) | NOT PEER-REVIEWED | Posted: 26 January 2025 doi:10.20944/preprints202501.1913.v1

Figure 16. Comparison of predicted and experimental values of the permeability coefficient at a water replenishment pressure of 0.01 kPa. The surface represents the predicted values, while the red dots denote the experimental results.

As observed in Figures 15 and 16, the predicted values of the soil permeability coefficient (represented by the surface plots) closely match the experimental values (denoted by the red dots) across all tests. Despite variations in the freezing boundary conditions—frozen temperature, cooling rate, and water replenishment pressure—the experimental data consistently align with the predicted surfaces. This demonstrates the robustness and reliability of the model, confirming its ability to predict permeability coefficients with high accuracy even when all three freezing boundary conditions are varied simultaneously.

These results highlight the model's practical application in real-world conditions and underscore its potential for use in predicting soil permeability under varying freezing conditions in AGF projects.

7. Conclusions

1. Effect of Cooling Rate on Permeability: The cooling rate plays a crucial role in determining the soil permeability coefficient. Specifically, as the cooling rate increases, the permeability coefficient of thawed soil decreases. This relationship underscores the importance of controlling the cooling rate in managing soil permeability in AGF projects. Understanding and manipulating this parameter can significantly impact soil thaw settlement following artificial freezing construction.
2. Coupling Effect of Temperature Gradient and Cooling Rate on Permeability: While an increase in cooling rate consistently leads to a reduction in soil permeability, the magnitude of this reduction is influenced by the temperature gradient. Specifically, the smaller the temperature gradient, the more pronounced the decrease in permeability for a given increase in the cooling rate. This coupled effect underscores the complexity of soil behavior under freezing conditions and highlights the need for an integrated approach when considering both temperature gradient and cooling rate in practice AGF projects.
3. Development of a Predictive Model: A predictive model for soil permeability has been developed based on a modified Kozeny-Carman equation, which incorporates the effects of cooling rate, temperature gradient, and water replenishment pressure. This model offers a robust and adaptable tool for predicting soil permeability across a range of environmental conditions. By accounting for multiple freezing boundary conditions, it provides deeper insights into the behavior of soils after open frozen.

Acknowledgements: This research was funded by the National Natural Science Foundation of China[grant number 41831278], Zhejiang Provincial Natural Science Foundation of China[grant number LY22E090003] and the Startup Fund of Shantou University [grant number NTF21015].

References

1. An, R., Kong, L., & Li, C. (2020). Pore Distribution Characteristics of Thawed Residual Soils in Artificial Frozen-Wall Using NMRI and MIP Measurements. *Applied Sciences, 10*(2), 544. Retrieved from https://www.mdpi.com/2076-3417/10/2/544
2. Bao, J., Xue, S., Zhang, P., Dai, Z., & Cui, Y. (2020). Coupled effects of sustained compressive loading and freeze–thaw cycles on water penetration into concrete. *Structural Concrete, 22*(S1), 11.
3. Chamberlain, E. (1990). Effect of freeze-thaw cycles on the permeability and macrostructure of soils. *Cold Region Research and Engineering Laboratory, 90*(1), 11.
4. Chen, C., Zhang, C., Liu, X., Pan, X., Pan, Y., & Jia, P. (2023). Effects of freeze-thaw cycles on permeability behavior and desiccation cracking of dalian red clay in china considering saline intrusion. *Sustainability, 15*(4), 20.

Preprints.org (www.preprints.org) | NOT PEER-REVIEWED | Posted: 26 January 2025 doi:10.20944/preprints202501.1913.v1

5. Chen, J., Tong, H., Yuan, J., Fang, Y., & Gu, R. (2022). Permeability prediction model modified on kozeny-carman for building foundation of clay soil. *Buildings, 12*(11), 1798.
6. Hirose, G., & Ito, Y. (2017). Experimental estimation of permeability of freeze-thawed soils in artificial ground freezing. *Procedia engineering, 189*, 332-337.
7. Hui, B., & Ping, H. (2009). Frost heave and dry density changes during cyclic freeze-thaw of a silty clay. *Permafrost and periglacial Processes, 20*(1), 65-70.
8. Joudieh, Z., Cuisinier, O., Abdallah, A., & Masrouri, F. (2024). Artificial Ground Freezing—On the Soil Deformations during Freeze–Thaw Cycles. *Geotechnics, 4*(3), 718-741. Retrieved from https://www.mdpi.com/2673-7094/4/3/38
9. Leonhardt, F. (1997). The committee to save the tower of Pisa: a personal report. *Structural engineering international, 7*(3), 201-212.
10. Li, Y., Yang, G., Ye, W., Li, J., Wang, G., & Wang, J. (2023). Deterioration law and microscopic mechanism of hydraulic characteristics of undisturbed loess in Ili under freeze-thaw action. *Journal of Engineering Geology, 31*(4), 8.
11. Lv, Q., Zhang, Z., Zhang, T., Hao, R., Guo, Z., Huang, X., . . . Liu, T. (2021). The Trend of Permeability of Loess in Yili, China, under Freeze–Thaw Cycles and Its Microscopic Mechanism. *Water, 13*(22), 19.
12. Ren, H., Hu, X.-d., Hong, Z.-q., & Zhang, J. (2019). Experimental study on active freezing scheme of freeze-sealing pipe roof used in ultra-shallow buried tunnels. *Chinese Journal of Geotechnical Engineering, 41*(2), 9.
13. Ren, X., Zhao, Y., Deng, Q., Kang, J., Li, D., & Wang, D. (2016). A relation of hydraulic conductivity—void ratio for soils based on Kozeny-Carman equation. *Engineering geology, 213*, 89-97.
14. Sun, C., Wang, P., Guo, H., Song, T., & Wang, H. (2024). Study on the influence of different temperature modes on the freezing characteristics of silty clay in seasonally frozen area under unidirectional freezing. *Journal of glaciology and geocryology, 46*(06), 1839-1848.
15. Viklander, P. (1998). Permeability and volume changes in till due to cyclic freeze-thaw. *Canadian Geotechnical Journal, 35*(3), 7.
16. Wang, X. (2009). Study on the property and the influence to surrounding environment of artificial freezing soil's thaw-settlement.
17. Wu, T. (2021). Experimental study on frost heave characteristics of soil under different freezing modes. *Journal of Zhongyuan University of Technology, 32*(02), 42-47.
18. Xu, J., Wang, Z., Ren, J., & Yuan, J. (2016). Experimental research on permeability of undisturbed loess during the freeze-thaw process Process. *Journal of Hydraulic Engineering, 47*(9), 10.
19. Yang, P., & Zhang, T. (2002). The Physical and the Mechanical Properties of Original and Frozen-Thawed Soil. *Journal of glaciology and geocryology, 24*(5), 3.
20. Zhang, H., Zhang, J.-m., Zhang, Z.-l., & Chai, M.-t. (2016). Measurement of hydraulic conductivity of Qinghai-Tibet Plateau silty clay under subfreezing temperatures. *Chinese Journal of Geotechnical Engineering, 38*(6), 6.
21. Zhang, L. (2022). Experimental study on effect of freeze-thaw cycle on strength of clay. *Qinghai Transportation Science and Technology, 34*(03), 5.
22. Zhang, L., Liao, Y., & Wang, D. (2023). Study on the Influence of Dry-wet and Freeze-thaw Cycles on Soil Permeability Coefficients. *Construction technology, 52*(9), 6.
23. Zhou, J., & Tang, Y. (2015). Artificial ground freezing of fully saturated mucky clay: Thawing problem by centrifuge modeling. *Cold Regions Science and Technology, 117*, 1-11.
24. Zhou, Y., & Zhou, G. (2012). Intermittent freezing mode to reduce frost heave in freezing soils—experiments and mechanism analysis. *Canadian Geotechnical Journal, 49*(6), 686-693.

Disclaimer/Publisher's Note: The statements, opinions and data contained in all publications are solely those of the individual author(s) and contributor(s) and not of MDPI and/or the editor(s). MDPI and/or the editor(s) disclaim responsibility for any injury to people or property resulting from any ideas, methods, instructions or products referred to in the content.